Chemical and biological sensors

Development of a Sub-10-ppm Limit of Detection Lateral Nanogap Gas Sensor

Sayali Tope[1], Seungbeom Noh[1], Rana Dalapati[2], Ling Zang[2], and Hanseup Kim[1]*

[1]*Electrical and Computer Engineering Department, University of Utah, Salt Lake City, UT 84112 USA*
[2]*Materials Science and Engineering Department, University of Utah, Salt Lake City, UT 84112 USA*
**Senior Member, IEEE*

Manuscript received 30 June 2023; revised 7 August 2023; accepted 8 August 2023. Date of publication 22 August 2023; date of current version 29 August 2023.

Abstract—This letter reports a wake-up gas sensor based on a lateral nanogap structure that is capable of increasing nanogap surface area by 11.2 times and thus improving the limit-of-detection (LOD) by 10 times down to 5 parts per million (ppm) in comparison with the previous vertical nanogap structure. Unlike the vertical nanogap structure with a suspended membrane, this lateral nanogap structure avoided fragile components and thus was able to reliably release a relatively large surface area of a 5-nm gap structure. The microfabricated lateral nanogap structure spanned over an enlarged area of 700 μm^2, in comparison with the maximum area of 62.5 μm^2 in the previous vertical gap structure, with the highest surface-area-to-nanogap-size aspect ratio of 130 μm^2/nm. When coated with a customized linker, it demonstrated (1) a gas sensing capability down to 5 ppm under the exposure of hexanal at a flow rate of 50 sccm, (2) a high wake-up ON current of 460 nA, and (3) an ON/OFF ratio of 1.51, which are sufficient for detection.

Index Terms—Chemical and biological sensors, electrochemical and gas sensors, atomic layer deposition (ALD) exposure mode, biomarker, conformality, hexanal, lateral nano-gap, limit of detection (LOD), ON/OFF ratio, sub-10-nm, sub-10-parts per million (ppm), volatile organic compounds (VOCs), wake-up gas sensor.

I. INTRODUCTION

A. Need for a Sub-10-Parts Per Million (ppm) LOD Gas Sensor

Detection of specific volatile organic compounds (VOCs) is increasingly finding its applications covering disease warning in humans and plants to food quality and safety surveillance. Specifically, among various VOCs, hexanal, an aldehyde, is regarded as a significant biomarker because it is emitted when plants are under stress [1], [2], [3]; when humans suffer from some inflammation [4], [5], lung cancers [3], [6], [7], [8], asthma [5], and chronic obstructive pulmonary disease (COPD); even when humans smoke or are exposed to indirect smoke within a certain period of time [5], [9], [10], and when foods, e.g., milk, degrade through oxidation [11]. Thus, the ability to detect a VOC, hexanal, would be a key technology that can contribute to human well-being.

To widely deploy such hexanal detection capabilities into a field, a wake-up gas sensor has been reported in an ultralow-power (<20 pW) design [12], wake-up threshold modulation [13], plant VOC detection [1], and crop damage detection in the actual sorghum fields [2]. Such a sub-10-nm wake-up nanogap gas sensor reported notable sub-nW power consumption, normally dormant operation, and detection of hexanal in 77.74 ppm in the actual sorghum field [1] and 50 ppm in the lab setting.

However, the current limit of detection (LOD) of such a wake-up gas sensor remains above 50 ppm and inherently restricts its use from numerous new applications as listed in Table 1. For example, the required LODs are 10, 5, and 0.005 ppm for the detection of indoor pollutants, milk degradation, and lung cancers. Thus, it is highly demanded to further lower the LOD of current wake-up gas sensors.

Corresponding author: Sayali Tope (email: sayali.tope@gmail.com).
Associate Editor: D. Uttamchandani.
Digital Object Identifier 10.1109/LSENS.2023.3307120

Table 1. Applications requiring sub-10-ppm hexanal LOD

Application	Required LOD
Insect damage stress in sorghum [1], [2]	10–50 ppm
Indoor pollutant and health hazard [9]	2–10 ppm
Milk quality [11]	5 ppm
Noninvasive lung cancer detection [14]	0.2–4.5 ppb
Hazelnut rancidity indicator [15]	0.25 ppb
COPD biomarker [10]	positive

B. Nanogap Area as a LOD Improvement Enabler

To lower the LOD further in a nanogap sensor, one can attempt to increase the nanogap area where gas molecules are temporarily captured and electrically bridge across the nanogap, as shown in our previous paper [13]. Fig. 1 depicts the concept of how a larger nanogap area leads to more molecular bridges, higher ON current, and thus a higher ON/OFF ratio for the same concentration of the exposed gas. The larger nanogap area can accommodate more molecular bridges to increase the ON current and provide a higher ON/OFF ratio in contrast to the relatively unchanging OFF current. Thus, to increase the ON/OFF ratio or to minimize the LOD, one can increase the nanogap area.

However, the maximum nanogap area is currently limited by the instability of the nanogap structure where a suspended cantilever forms a nanogap to the fixed electrode on the substrate. The exact position of a suspended cantilever structure can be subjected to variable stresses depending on the length, width, and thickness, as well as the interfacial stiction forces, such as capillary, electrostatic, and van der Waals [16], [17]. Currently, it was found that the maximum nanogap area for a sub-10-nm nanogap that was successfully released in our laboratory was 62.5 μm^2 due to the cantilever collapse [13].

The enhanced sizes of a large nanogap area can be microfabricated when one avoids the vertically suspended structure and instead utilizes a lateral structure. Recently, the authors demonstrated a new

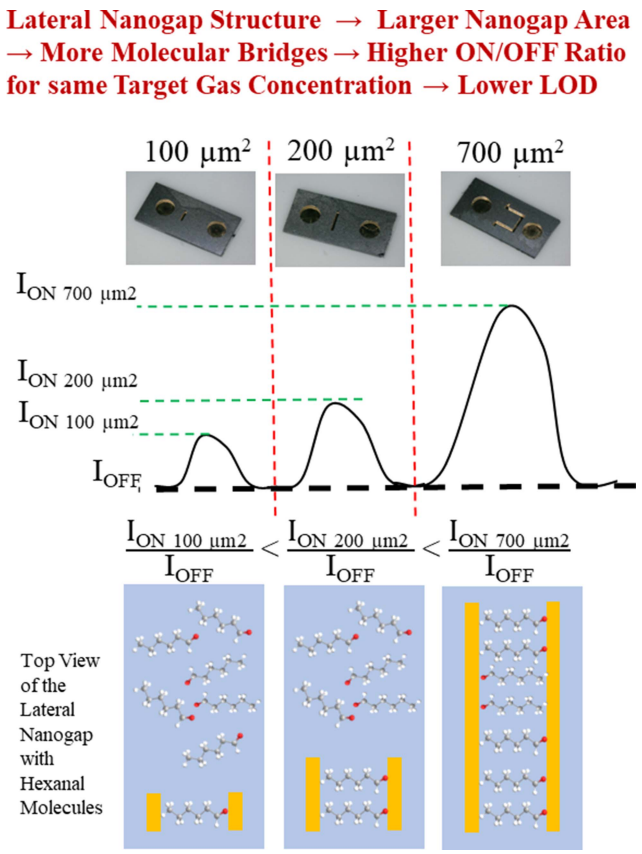

Fig. 1. Depiction of how a larger nanogap area leads to more molecular bridges and hence a lower LOD.

microfabrication method to construct a lateral sub-10-nm nanogap with a high conformality of 90.54% by manipulating the exposure mode deposition in the atomic layer deposition (ALD) technique [18].

In this letter, we report the use of such a sub-10-nm conformal lateral nanogap to enable enhanced nanogap area and achieve the lowering of LOD below 10 ppm for hexanal detection. Specifically, we report the fabrication process, testing procedures, and results.

II. FABRICATION PROCESS

Fig. 2(a) illustrates the fabrication process flow to construct a lateral nanogap sensor. First, on an oxidized silicon wafer, a 1 nm adhesive chromium (Cr) layer and 200 nm of gold (Au) layer were deposited and patterned to fabricate the first bottom electrode (step 1). On top of the patterned electrode, a sacrificial layer of Al_2O_3 was deposited by utilizing ALD to secure conformal film thicknesses (step 2). This conformal coating is the most critical step of this fabrication as it requires high precision in a 0.1 nm scale and determines the nanogap distance. It was achieved by employing the recently developed exposure mode ALD method in [1] for a 5.5-nm thick conformal Al_2O_3 layer on the sidewall of a 3-D nanostructure. Next, the second gold electrode was microfabricated in an identical way to the first electrode (step 3). Since the second electrode could not be perfectly aligned with current lithography equipment, it tends to cover a portion of the first electrode over the intended lateral gap structure on the front side of a wafer. To address this issue, the latter part of the fabrication was performed on the backside of the wafer. First, a passivation film of 50-μm thick Parylene-C was deposited to protect the devices from the subsequent Bosch and Al_2O_3 wet etching in the next steps (step 4). Then, the substrate was selectively etched to expose the gold in the vicinity of the nanogaps from the back side of the wafer. Here, the utilized back-side fabrication can be avoided by removing the overhand of the second electrode with the help of high-precision chemical mechanical polish or wet etching techniques in the future. Finally, the sacrificial layer of Al_2O_3 was etched in KOH at 80 °C to release the nanogaps. Fig. 2(b) shows the successfully fabricated lateral nanogap between two vertical electroplated gold electrodes, of which the cross-section was imaged by SEM. It clearly shows the targeted 5.5-nm nanogap distance in a lateral gap form.

The microfabricated devices were coated with specially synthesized conductive linker DB-PTCDI, which consists of two thiol groups. Note that gold was selected as an electrode material to guarantee strong thiol bonding of linkers to the electrode between the nanogap considering the linker chemistry. The second thiol group forms hydrogen bonding with the -CHO functional group of Hexanal. The molecular bridge formed by the linker and captured target molecules forms a conductive path between the two electrodes and drops the electrical impedance across the nanogap. As shown by the working principle in Fig. 3(a), the gas sensor switches from OFF to ON when target gas molecules were captured, and the ON current increases significantly compared with OFF current. Fig. 3(b) shows the 3-D view of the lateral nanogap device. Note that the previous vertical nanogap sensor demonstrated selectivity of >6.0 compared with alcohol, alkane, ketone, and phenyl functional groups [19].

III. GAS SENSOR TESTING METHODOLOGY

A. LOD Testing

To validate the hypothesis that a larger nanogap area leads to a lower LOD, the ON/OFF current ratios of a nanogap gas sensor were monitored utilizing 4200A-SCS, Keithley while lowering the hexanal exposure concentrations from 50 to 2.5 ppm. For nonconductive molecules, a capacitive detection scheme can be utilized. Fig. 4 shows the sub-10-ppm testing setup where the concentrations of hexanal were controlled by injecting the controlled volume of the liquid hexanal with a syringe with the smallest measurable volume of 50 nl into nitrogen as a dilution gas. The corresponding values of 2.5, 5, 10, and 50 ppm were calculated by injecting volumes of 50, 100, 200 nl, and 1 μl of pure liquid hexanal in 36 l of nitrogen.

The number of moles in 50 nl of liquid hexanal was given by

$$\text{Target Amount (mol)} = \frac{\text{Volume (l)} \times \text{Density}\left(\frac{\text{g}}{\text{l}}\right)}{\text{Molecular Weight}\left(\frac{\text{g}}{\text{mol}}\right)}$$

$$= \frac{50 \times 10^{-9}\,(\text{l}) \times 814\left(\frac{\text{g}}{\text{l}}\right)}{100.16\left(\frac{\text{g}}{\text{mol}}\right)} = 0.4064 \times 10^{-6}\ \text{mol}.$$

The 40 l Tedlar bag was filled to 90% of its capacity to avoid leakage and/or bursting of the bag. Thus, the number of moles in 36 l (90% of 40 l) of nitrogen was 0.1584 (1 l of nitrogen = 0.0044 moles).

The ppm of 50 nl of liquid Hexanal in 36 l of Nitrogen gas was calculated using the following formula:

$$\text{PPM} = \frac{\text{Target Amount}}{\text{Total Amount}} = \frac{0.4064 \times 10^{-6}\ \text{mol}}{0.1584\ \text{mol}} = 2.56\ \text{PPM}.$$

Using a Markes ACTI-VOC low flow gas sampling pump, the prepared gas sample was flown into a closed testing chamber with 50 sccm flow rate. The threshold ON/OFF ratio was set considering the baseline drift that was calculated by averaging the noise floor of the

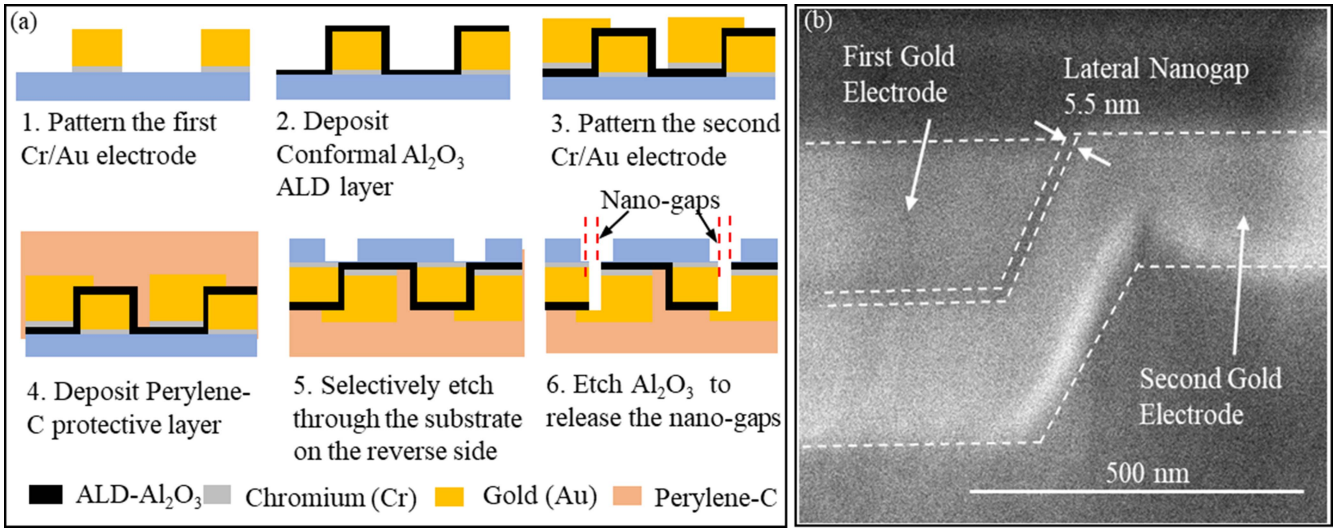

Fig. 2. (a) Cross-section view of the steps of the fabrication process flow. (b) SEM of the cross section of the 5.5 nm lateral nanogap device.

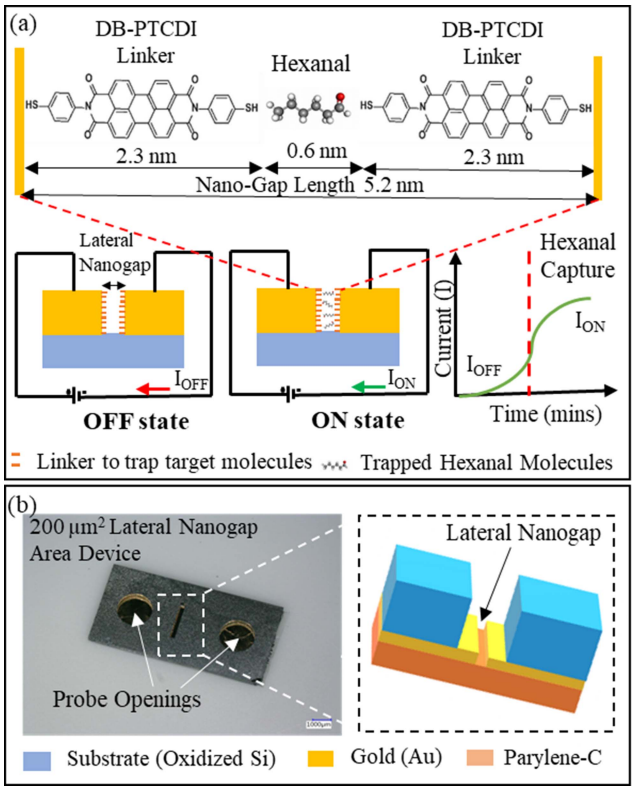

Fig. 3. (a) Working principle of a wake-up-based lateral nanogap sensor. (b) 3-D view of the lateral nanogap structure.

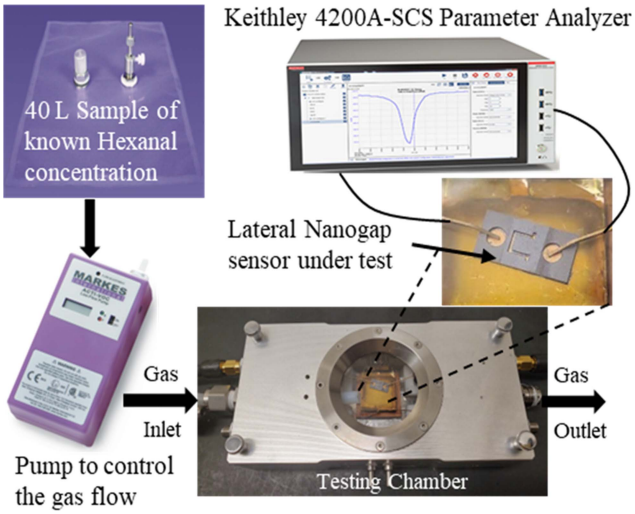

Fig. 4. Testing setup for sub-10-ppm lateral nanogap gas sensor with flow control using a pump, a closed testing chamber, and measurements using a parameter analyzer.

sensor output under inert gas flow, nitrogen, into the testing chamber for 1 h. The devices were tested for 50, 10, 5, and 2.5 ppm to measure the ON/OFF ratios at each concentration and determine the LOD.

B. Repeatability Testing

To verify the repeatability of the LOD detection, the same 700 µm^2 nanogap area device was exposed to the repeated injection pattern of 5 ppm hexanal concentration for 15 min followed by 15 min of nitrogen purging until the sensor no longer recovered, resulting in a permanent failure. The response in each repeatability cycle was considered a successful detection only if the ON/OFF ratio was above the noise floor measured in LOD testing.

IV. EXPERIMENTAL RESULTS

A. LOD Testing

The maximum nanogap area of 700 µm^2 showed the improved LOD down to 5 ppm compared to the previous suspension membrane nanogap results of 50 ppm LOD for 62.5 µm^2 nanogap area, hence validating the hypothesis that the larger nanogap area enables lower LOD. The baseline noise floor ON/OFF ratio was measured at 1.09 without any trigger. The sensor detection with ON/OFF ratios of 1.61, 1.52, and 1.51 for 50, 10, and 5 ppm hexanal concentrations was observed as shown in Fig. 5. The 2.5 ppm hexanal concentration did

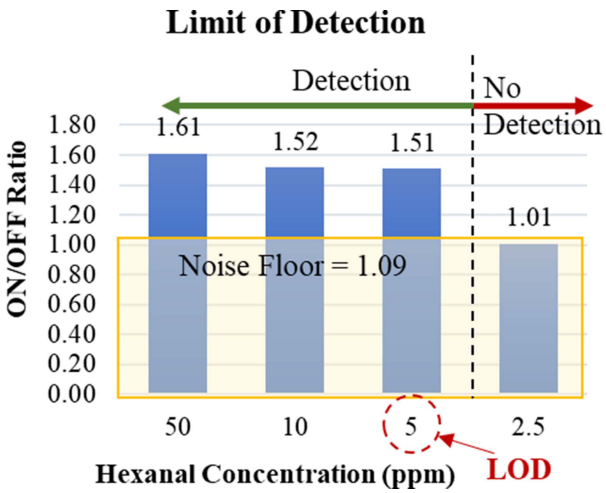

Fig. 5. For a 700 μm^2 nanogap area device, the LOD measured was 5 ppm. No detection was observed for sub-5-ppm.

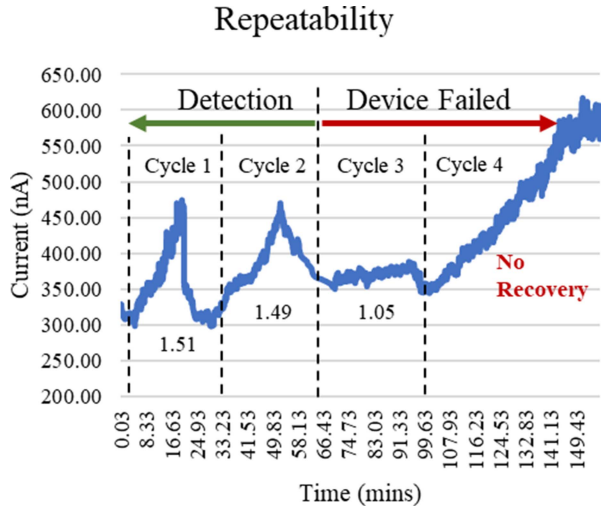

Fig. 6. Repeatability of the lateral nanogap sensor for four cycles of 5 ppm hexanal exposure and purging.

not show an acceptable ON/OFF ratio and remained below noise floor at ON/OFF ratio of 1.01. Thus, the LOD of the 700 μm^2 lateral nanogap sensor was measured as 5 ppm.

B. Repeatability Testing

The 5 ppm LOD detection repeatability of the 700 μm^2 nanogap area device was measured to be two at this point for an initial device after four cycles of sequential hexanal exposure and purging. Fig. 6 shows in the first cycle, the OFF current of 305 nA increased to an ON current of 460 nA resulting in an ON/OFF ratio of 1.51. Cycle 2 showed a slightly decreased ON/OFF ratio of 1.49. In cycle 3, the ON/OFF ratio dropped below the noise floor to 1.05 and was not identified as true detection. In the 4th cycle, the device did not recover, and the resistance kept dropping. It is hypothesized that such limited repeatability was caused by random particle landing and permanent bonding between a target gas molecule and linkers. Thus, we believe that repeatability can be improved by incorporating mesh packaging and high-voltage molecular burning functions in the future.

V. CONCLUSION

This letter reported the use of the previously microfabricated lateral nanogap structures to lower the hexanal detection LOD. The measurement results confirmed that an 11.2 times larger area from 62.5 to 700 μm^2 led to an improved LOD from 50 to 5 ppm. The microfabricated lateral nanogap device also demonstrated some repeatability for two cycles.

ACKNOWLEDGMENT

This work was supported by the cooperative agreement of the ARPAE OPEN 2018 Program under Grant DE-AR0001064 [Program Manager: Dr. Olga Blum Spahn (Previously Dr. David Babson)]. Microfabrication was performed at the state-of-the-art Utah Nanofabrication Facility at the University of Utah.

REFERENCES

[1] S. H. Khan et al., "Development of a gas sensor for green leaf volatile detection," in *Proc. 21st Int. Conf. Solid-State Sensors, Actuators Microsystems (Transducers)*, 2021, pp. 250–253.
[2] S. H. Khan et al., "Field deployment of a nanogap gas sensor for crop damage detection," in *Proc. IEEE 35th Int. Conf. Micro Electro Mech. Syst. Conf.*, 2022, pp. 720–723.
[3] P. Fuchs et al., "Breath gas aldehydes as biomarkers of lung cancer," *Int. J. Cancer*, vol. 126, pp. 2663–2670, 2010.
[4] L. M. Müller-Wirtz et al., "Differential response of pentanal and hexanal exhalation to supplemental oxygen and mechanical ventilation in rats," *Molecules*, vol. 26, 2021, Art. no. 2752.
[5] A. M. Maria et al., "Volatile organic compounds in COPD: Is hexanal an inflammation biomarker?," *Eur. Respir. J.*, vol. 48, Sep. 2016, Art. no. PA4412.
[6] M. A. Floss et al., "Exhaled aldehydes as biomarkers for lung diseases: A narrative review," *Molecules*, vol. 27, no. 16, 2022, Art. no. 5258.
[7] D. Poli et al., "Determination of aldehydes in exhaled breath of patients with lung cancer by means of on-fiber-derivatisation SPME-GC/MS," *J. Chromatography B.*, vol. 878, pp. 2643–2651, 2010.
[8] P. Wang et al., "Identification of lung cancer breath biomarkers based on perioperative breathomics testing: A prospective observational study," *EClinicalMedicine*, vol. 47, 2022, Art. no. 101384.
[9] L. Ernstgård et al., "Acute effects of exposure to hexanal vapors in humans," *J. Occup. Environ. Med.*, vol. 48, no. 6, pp. 573–580, 2006.
[10] M. Corradi et al., "Aldehydes in exhaled breath condensate of patients with chronic obstructive pulmonary disease," *Amer. J. Respir. Crit. Care Med.*, vol. 167, pp. 1380–1386, 2003.
[11] M. Asaduzzaman et al., "Hexanal as biomarker for milk oxidative stress induced by copper ions," *J. Dairy Sci.*, vol. 100, no. 5, May 2017, Art. no. 4193.
[12] S. H. Khan et al., "Characterization of a wake-up nano-gap gas sensor for ultra low power operation," *J. Microelectromech. Syst.*, vol. 31, no. 5, pp. 791–801, Oct. 2022.
[13] S.-U. H. Khan et al., "Threshold point modulation of a wake-up nano-gap gas sensor," in *Proc. IEEE 33rd Int. Conf. Micro Electro Mech. Syst.*, 2020, pp. 733–736.
[14] A. Ulanowska et al., "The application of statistical methods using VOCs to identify patients with lung cancer," *J. Breath Res.*, vol. 5, 2011, Art. no. 46008.
[15] S. Pastorelli et al., "SPME analytical method for the determination of hexanal in hazelnuts as indicator of the interaction of active packaging materials with food aroma compounds," *Food Additives Contaminants*, 2006, vol. 23, no. 11, pp. 1236–1241.
[16] N. Tas et al., "Stiction in surface micromachining," *J. Micromechanics Microengineering*, vol. 6, 1999, Art. no. 385, doi: 10.1088/0960-1317/6/4/005.
[17] M. Tilli et al., "*Handbook of Silicon-Based Mems Materials and Technologies*. Amsterdam, The Netherlands: Elsevier, 2015.
[18] S. Tope, S. Noh, and H. Kim, "Wafer-level fabrication of conformal sub 10-NM nanogaps," in *Proc. IEEE 36th Int. Conf. Micro Electromechanical Syst.*, 2023, pp. 657–660.
[19] S. H. Khan, "Development, characterization and field deployment of a near-zero-power gas sensor (16419)," Ph.D. dissertation, Univ. Utah, 2022.